Thermodynamic Analysis of A Carbon Neutral Polygeneration System with Solar Chemical Looping Dry Reforming and Photovoltaic Electrolysis

Shiying Yang[1,2], Fan Jiao[1,2], Yibiao Long[1,2], Xiangyu Yan[1,3], Taixiu Liu[1,2], Qibin Liu[1,2*]

1 Institute of Engineering Thermophysics, Chinese Academy of Sciences, Beijing 100190, P.R. China

2 University of Chinese Academy of Sciences, Beijing, 100049, P.R. China

3 International Research Center for Renewable Energy & State Key Laboratory of Multiphase Flow in Power Engineering, Xi'an

Jiaotong University, Xi'an, 710049, China

(*Qibin Liu: qibinliu@iet.cn)

ABSTRACT

Distributed energy supply involving solar energy is a promising way to improve sustainable development. However, the challenges of high energy consumption for CO_2 capture and low solar share in traditional solar natural gas reforming or coal gasification polygeneration still need to be overcome. Here, we proposed a novel solar carbon-neutral polygeneration system integrated with solar chemical looping dry reforming, PV-SOEC and distributed energy supply, characterized by enhanced solar share, low carbon capture energy consumption and high efficiency. The used solar chemical looping dry reforming not only obtains automatic separation products of CO and H_2, but upgrade solar energy into chemical energy. The obtained CO combined with the by-product of PV-SOEC (O_2) is then used for generation on the way of pure oxygen combustion. The exhausted CO_2 is cascaded utilized through an absorption refrigeration and heat exchange, and then captured with no extra energy consumption. Through a simulation model, we find that the overall system efficiency can reach 63.7% with a solar share of 44.2%. The solar-to-chemical efficiency of the solar chemical looping dry reforming unit is 63.9%. This work offers a promising solution for the integration and construction of a high-efficiency, high-solar-share energy system.

Keywords: hydrogen, solar energy, carbon neutrality, solar thermochemical conversion, polygeneration

NONMENCLATURE

Abbreviations	
STC	Solar Thermochemical Conversion
SMR	Steam methane reforming
CLDR	Chemical Looping Dry Reforming
RB	Reverse Boudouard
CMD	Catalyst Methane Decomposition
SOEC	solid oxide electrolysis cell
PDC	parabolic dish collector
ICE	internal combustion engine
COP	coefficient of performance
VOP	Voltage Overpotential

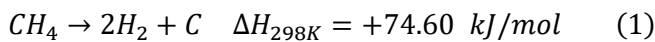| Symbols	
h_{PV}	convection coefficient of PV cell
σ	Stefan-Boltzmann constant
F	Faraday constant
λ	wave length
ε_{PV}	emissivity of PV cell
J_{SC}	short-circuit current density
V_{OC}	open circuit voltage
FF	fill factor

1. INTRODUCTION

The development of the society is intricately linked with energy utilization, but excessive exploitation of fossil fuels has led to serious environmental pollution and carbon emission. Hydrogen, with a high energy density and clean combustion property, offers an ideal energy substitute. However, predominant hydrogen production methods rely on fossil fuels, posing

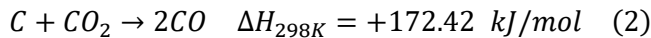significant pollution and carbon dioxide emission challenges.

Solar energy, as the most potential renewable energy, has attracted much attention. Integrating solar energy with fossil fuels for hydrogen production optimizes renewable resource utilization and diminishes the dependence on fossil energy. The emergence of solar thermochemical conversion (STC) presents an innovative solution for clean fuel production.

Among the conventional technologies of producing clean fuels from fossil fuels [1, 2], steam methane reforming (SMR) yields a portion of syngas, but faces challenges such as non-separability of the product, high energy consumption and significant pollution. Super-dry reforming [3] achieves carbon dioxide enrichment through the use of CO2 sorbent, but is limited by the complex catalyst preparation process. Although methane decomposition exhibits excellent gas-solid separation characteristics[4, 5], it is plagued by carbon deposition during the reaction, affecting overall performance.

CMD:
$$CH_4 \rightarrow 2H_2 + C \quad \Delta H_{298K} = +74.60 \ kJ/mol \quad (1)$$
RB:
$$C + CO_2 \rightarrow 2CO \quad \Delta H_{298K} = +172.42 \ kJ/mol \quad (2)$$

At present, a novel chemical looping dry reforming (CLDR) technology, with automated product separation for clean fuel production, has gained significant attention. The method comprises a two-step reaction in Eqs. (1) and (2). The first step involves the CMD reaction for hydrogen production, while in the second step, carbon serves as a reactant in the RB reaction, facilitating carbon monoxide production and eliminating carbon deposition. Takenaka et al.[6] introduced this concept in 2004, while More and Veser et al. [7, 8] explored its circulation effects and different heating methods are studied from the system level.

Based on the above methods, we propose a novel solar driven carbon-neutral polygeneration system, which integrates cooling, heating and power supply. The key contributions of this study are:

(1) A numerical model for the zero-carbon emission polygeneration system is proposed, and each subsystem is numerically analyzed.
(2) The performance of the hydrogen production subsystem under different DNIs is studied, and the fuel yield and performance of Solar-CLDR unit and PV-SOEC unit are evaluated.
(3) The overall performance of the zero-carbon polygeneration system, including its operational efficiency and production under typical solar irradiation conditions, is evaluated.

2. MODEL DEVELOPMENT AND EVALUATION CRITERIA

2.1 Schematic of novel system

The innovative solar carbon-neutral polygeneration system comprises four units: concentrated solar chemical looping dry reforming (Solar-CLDR) hydrogen generation unit, photovoltaic-solid oxide electrolysis cell (PV-SOEC) hydrogen generation unit, internal combustion engine (ICE) pure oxygen combustion power generation unit and the double-effect Li-Br absorption refrigeraton unit. The schematic of the proposed system is shown in Fig.1.
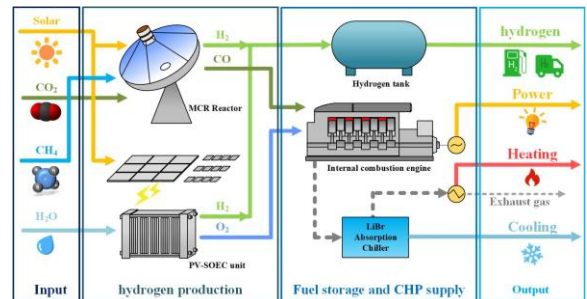

Fig. 1. Schematic of the proposed system

The Solar-CLDR unit and PV-SOEC unit constitute the hydrogen production module, enabling the production of hydrogen fuel and obtaining accessible carbon monoxide fuel and oxygen. The CO is utilized for electricity generation by pure oxygen combustion in the ICE. The waste heat of CO_2 from the ICE exhausted gas is comprehensively utilized to provide both heating and cooling by integrated with absorption refrigerator. Table 1 presents the normal parameters for the proposed system.

Table 1. normal parameters for the system

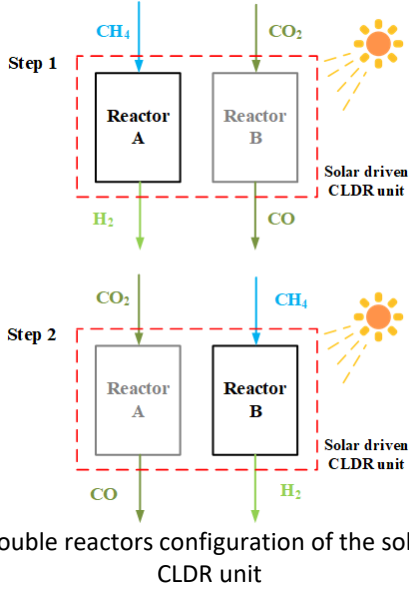| Parameters	Value
Direct nominal Irradiation (W/m2)	800
Total area of the solar collector (m²)	600
Total area of the photovoltaic cell (m²)	650[9]
Electrical efficiency of the ICE (kW)	37.3%
COP of the LiBr absorption refrigerator	1.26

2.2 Solar driven CLDR unit

Fig. 2. Double reactors configuration of the solar driven CLDR unit

In the solar driven CLDR unit, solar irradiation is initially focused through a parabolic dish collector (PDC), and then introduced into the solar thermochemical reactor, driving the thermochemical reaction. The concentrated solar energy utilized in this process can be calculated by

$$E_{sol-CLDR} = DNI \cdot A_{PDC} \cdot \eta_{dish-opt} \cdot \eta_{heat} \quad (3)$$

where $\eta_{dish-opt}$ and η_{heat} are the average optical efficiency of the collector and heat efficiency of the reactor, respectively.

In this study, we use the configuration of double reactors, and staggered the reaction steps between the two reactors. As shown in the Fig.2, the CMD reaction alternates with the RB reaction in two reactors, achieving continuous and separate acquisition of H_2 and CO.

2.3 PV-SOEC unit

In the PV module, only part of the solar energy can be utilized, corresponding to the photon energy above the band gap of the PV cells, which can be calculated by:

$$E_{sol-PV} = DNI \cdot A_{PV} \cdot \frac{\int_{280}^{\lambda_g} E_\lambda \, d\lambda}{E_{spectrum}} \quad (5)$$

The energy balance in the PV module is given[10]:

$$E_{sol-PV} = E_{PV-optloss} + P_{out} + Q_{heatloss} + Q_{fluid} \quad (6)$$

The optical loss ($E_{PV-optloss}$) and the heat loss ($Q_{heatloss}$) of the PV module are given by:

$$E_{PV-optloss} = E_{sol-PV} \cdot (1 - \eta_{opt}) \quad (7)$$

$$Q_{heatloss} = h_{PV} \cdot (T_{PV} - T_0) + \varepsilon_{PV} \cdot \sigma \cdot (T_{PV}^4 - T_0^4) \quad (9)$$

The electricity generating capacity of PV cells can express by[11]:

$$P_{out} = J_{sc} \cdot V_{oc} \cdot FF \quad (10)$$

In the SOEC module, the reactant water undergoes electrolysis and yields H_2 and O_2.

The hydrogen quantity produced at the SOEC cathode interface can be determined by:

$$n_{H_2-SOEC} = \frac{J}{2F} \quad (11)$$

The operation voltage of the SOEC, as known as the Voltage Overpotential (VOP), can be calculated by :

$$VOP = E + V_{act} + V_{ohm} + V_{conc} \quad (13)$$
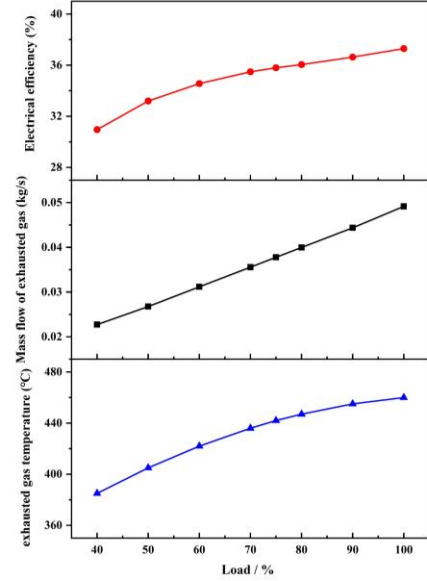
2.4 Power generation unit

Fig. 3 electricity efficiency, mass flow rates, and exhaust gas temperatures of ICE at various loads

In this module, oxygen generated by SOEC and carbon monoxide fuel from the CLDR unit are fed into the internal combustion engine (ICE) for electricity production. The performance of ICE at various loads was shown in Fig.3[12].

2.5 Double-effect Li-Br absorption refrigeration unit

In order to achieve cascade utilization of energy, the waste heat from the ICE is used to drive a absorption refrigerator[13]. The cooling output C can
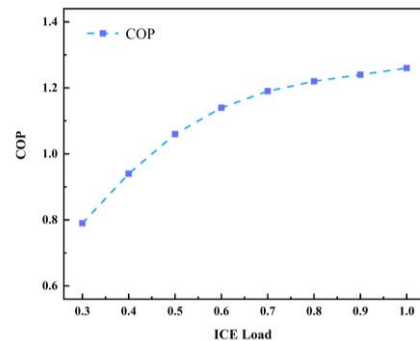

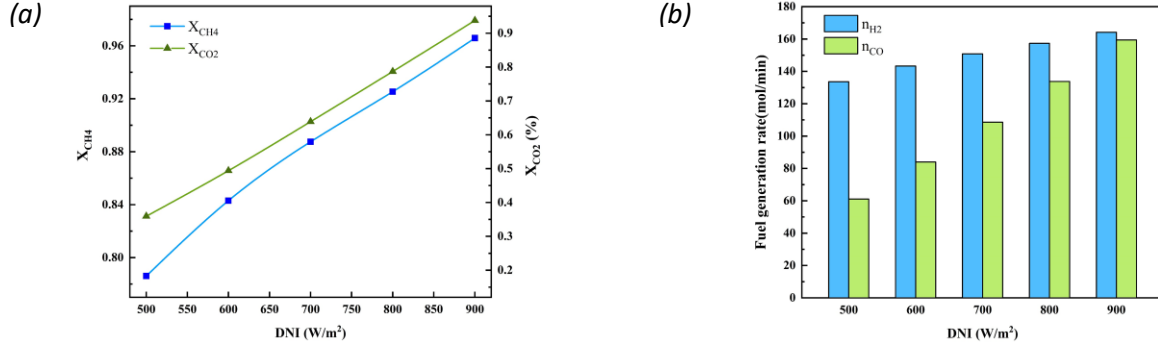Fig.4 COP of the refrigerator under different ICE load

Fig. 5 (a) the conversion rate of CH₄ and CO₂; (b) the production of H₂ and CO in the CLDR unit under varied DNI

be calculated by:

$$C = COP \cdot Q_{HPG} \qquad (14)$$

where Q_{HPG} represents the heat recovered by the chiller. The COP under different ICE loads is illustrated in Fig.4.

2.6 Evaluation criteria

The thermodynamic performance of the overall system and subsystem was evaluated using these criteria.

(1) Energy efficiency of the CLDR-PV-SOEC subsystem

$$\eta_{en} = \frac{HHV_{H_2} \cdot n_{H_2} + HHV_{CO} \cdot n_{CO}}{Q_{sol} + Q_{sol-2} + HHV_{CH_4} \cdot n_{CH_4}} \qquad (15)$$

(2) Exergy efficiency of the CLDR-PV-SOEC subsystem

$$\eta_{ex} = \frac{Ex_{H_2} \cdot n_{H_2} + Ex_{CO} \cdot n_{CO}}{A_{sol}(Q_{sol-1} + Q_{sol-2}) + Ex_{CH_4} \cdot n_{CH_4}} \qquad (16)$$

(3) Solar-to-chemical efficiency of the CLDR process

$$\eta_{sol-chemical} = \frac{Q_{sol-chem}}{Q_{sol}}$$
$$= \frac{n_{CH_4} \cdot X_{CH_4} \cdot \Delta_r H_{CMD} + n_{CO_2} \cdot X_{CO_2} \cdot \Delta_r H_{RB}}{Q_{sol-1}} \qquad (18)$$

(4) Solar share

$$\lambda = \frac{Q_{sol}}{Q_{total-input}} = \frac{Q_{sol-1} + Q_{sol-2}}{Q_{sol-1} + Q_{sol-2} + HHV_{CH_4} \cdot n_{CH_4}} \qquad (19)$$

(5) Energy efficiency of the overall system

$$\eta_{en-total} = \frac{Q_{fuel} + P + C + Q_{heat}}{Q_{sol-1} + Q_{sol-2} + HHV_{CH_4} \cdot n_{CH_4}} \qquad (20)$$

3. RESULTS AND DISCUSSION

3.1 Performance analysis

3.1.1 Solar driven CLDR unit

As DNI increases, the solar collector receives more energy, which drives both CMD and RB reactions. Fig.5-a illustrates that higher DNIs result in the increased conversion rates in both reactions.

Fig.5-b presents the specific production of hydrogen and carbon monoxide fuel under varying DNIs. When the DNI is 900, the carbon dioxide conversion reaches 93.8%, and the methane conversion reaches 96.6%. The production of hydrogen and carbon monoxide reaches 164.2 and 159.4 mol/min

3.1.2 PV-SOEC unit

The energy distributions of PV module under varying DNI conditons are examined, as shown in Fig.6-a. As DNI rises from 500 to 900 W/m2, P rises to 128.4 kW, with an increase of 84.9%.

In this study, we investigate the impact of various electricity inputs (attributed to different DNI levels) on
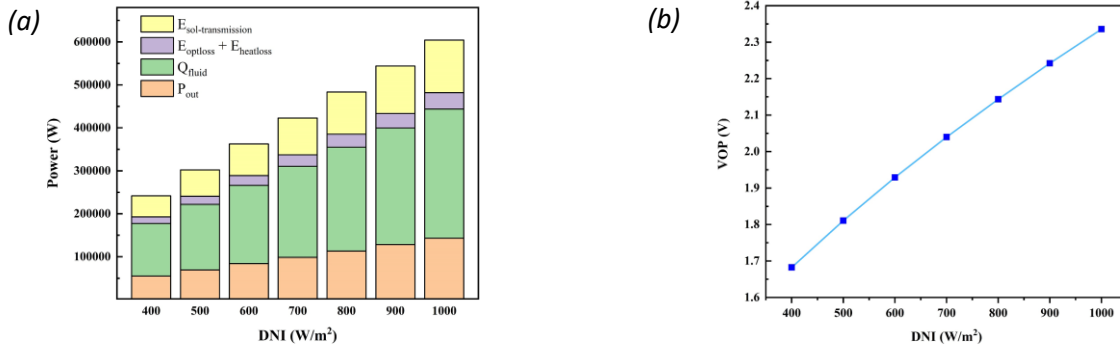

Fig. 6 (a) energy distribution of PV module; (b) VOP of the SOEC module under varied DNI
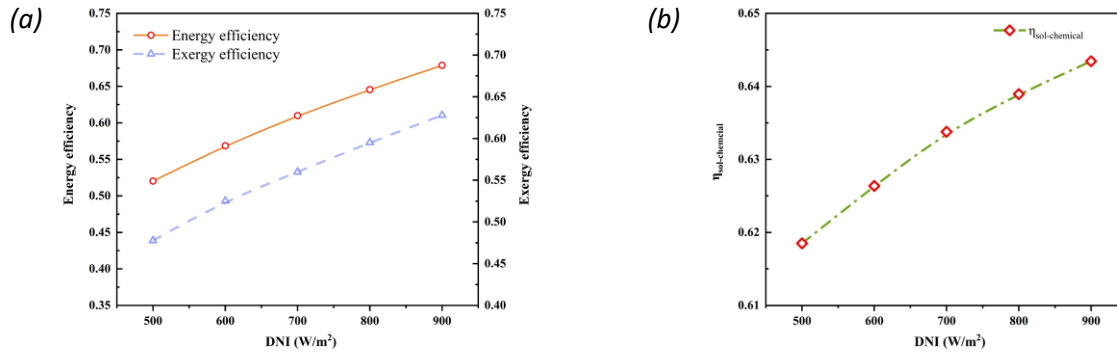
Fig. 7 (a) Energy efficiency and exergy efficiency of the hydrogen production subsystem; (b) Solar-to-chemical efficiency of the CLDR process under different DNI

the output of the SOEC module. The VOP of the SOEC is illustrated in Fig.6-b. With the increase of DNI, the value can reach 2.24 V when DNI reaches 900.

3.1.3 Solar-CLDR-PV-SOEC subsystem's performance

The hydrogen production module comprises the solar driven CLDR unit and the PV-SOEC unit. Fig.7 illustrates the energy efficiency and exergy efficiency of the hydrogen production subsystem and the solar-to-chemical efficiency of CLDR unit.

Both the energy efficiency and exergy efficiency of the subsystem increases with the DNI. At 900 W/m², the η_{en} and η_{ex} reach 67.9% and 62.8%, respectively. The CLDR process has a solar-to-chemical efficiency of 64.3% at 900 DNI, which is 10% point higher than the conventional concentrated solar DMR process[14]

3.1.4 overall polygeneration system's performance

Based on the above subsystems, we construct a polygeneration system. We analysize the system's performance under various ICE loads and DNIs. As shown in Fig.8, when the ICE load changes from 100% to 50%, the energy efficiency can remain relatively stable (63.9% to 63.5%). When the DNI changes from 200 to 900, the energy efficiency can reach 66.9%, with a high solar share of 47.1%.

The polygeneration capacity of the system under specified condition is also presented. As shown in Fig.9, the chemical energy of hydrogen and carbon monoxide fuel is 827 and 557 kW, respectively. Additionally, it provides 28 kW of power, 10 kW of heating output, and 17 kW of cooling output. The system achieves an energy efficiency of 63.7% and a high solar share of 44.2%.

4. CONCLUSIONS

To tackle with the problems of high energy consumption for CO_2 capture and low solar share in tradional polygeneration systems (just like solar nature gas reforming or coal gasification system). we proposed a novel solar carbon-neutral polygeneration system in this study.

In this system, the combination of solar chemical dry reforming (Solar-CLDR) unit and photovoltaic solid oxide electrolysis cell (PV-SOEC) unit can achieve the synthesis and auto separation of clean fuel. The integration of pure oxygen combustion power generation and absorption refrigeration enables the carbon capture without energy penlty. The carbon dioxide can be recycled and act as the reactant in the CLDR process, resulting in a net zero carbon emission for the entire system. The research findings are summarized as follows:
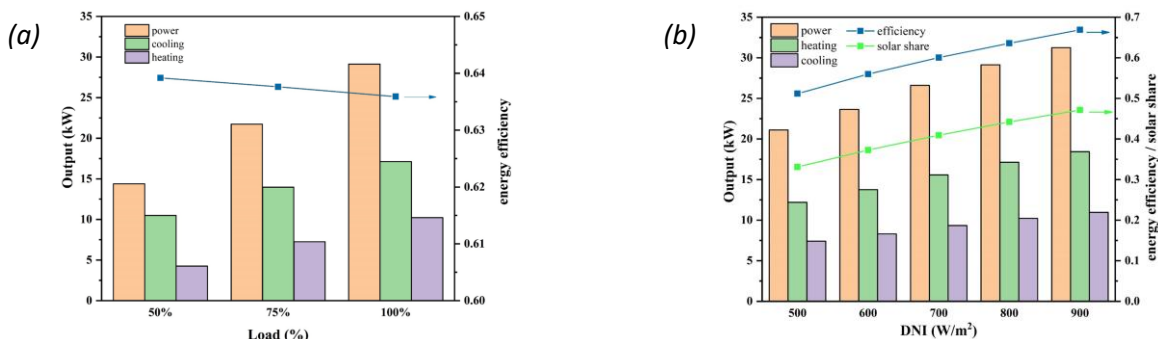

Fig. 8 (a)Energy efficiency and various output of the polygeneration system under different ICE loads; (b) Energy efficiency, solar share and various output of the polygeneration system under different DNI values
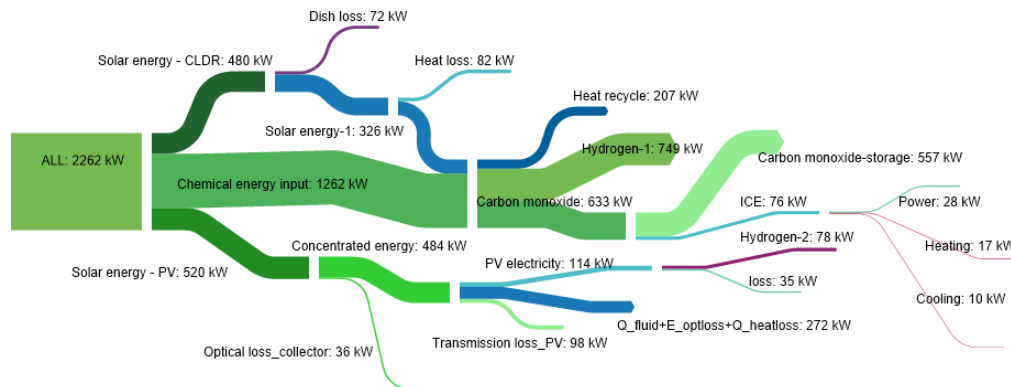
Fig. 9 Total energy distribution of the polygeneration system

1. By conbining the solar chemical looping dry reforming process with the photovoltaic hydrogen production process, the system improves the share of renewable energy in the overall system compared to traditional technologies. At the same time, the coupling of Solar-CLDR unit and PV-SOEC unit also realizes the efficient fuel production of the whole system.

2. The energy and exergy efficiencies of the hydrogen production subsystem are 64.55% and 59.52%, respectively, and the solar-to-chemical efficiency of the CLDR process is 64.3%, which is nearly 10% points higher than that of traditional concentrated solar methane dry reforming.

3. Under specified conditions, the polygeneration system attains an 63.7% of energy efficiency and a 44.2% of solar share. The variability of product caters to different energy requirements such as hydrogen production stations or hydrogen refueling stations.

DECLARATION OF INTEREST STATEMENT

The authors declare that they have no known competing financial interests or personal relationships that could have appeared to influence the work reported in this paper. All authors read and approved the final manuscript.

REFERENCE

[1] C. Acar and I. Dincer, "Comparative assessment of hydrogen production methods from renewable and non-renewable sources," *International Journal of Hydrogen Energy,* vol. 39, no. 1, pp. 1-12, 2014/01/02/ 2014.

[2] D. Pashchenko, "Integrated solar combined cycle system with steam methane reforming: Thermodynamic analysis," *International Journal of Hydrogen Energy,* vol. 48, no. 48, pp. 18166-18176, 2023/06/05/ 2023.

[3] L. C. Buelens, V. V. Galvita, H. Poelman, C. Detavernier, and G. B. Marin, "Super-dry reforming of methane intensifies CO2 utilization via Le Chatelier's principle," *Science,* vol. 354, no. 6311, pp. 449-452, Oct 2016.

[4] J. Raza *et al.*, "Methane decomposition for hydrogen production: A comprehensive review on catalyst selection and reactor systems," *Renewable and Sustainable Energy Reviews,* vol. 168, p. 112774, 2022/10/01/ 2022.

[5] Y. F. Li, H. S. Yu, X. H. Jiang, G. R. Deng, J. Z. Wen, and Z. C. Tan, "Techno-economic analysis for hydrogen-burning power plant with onsite hydrogen production unit based on methane catalytic decomposition," *Energy Conversion and Management,* vol. 277, Feb 2023, Art. no. 116674.

[6] S. Takenaka, Y. Tomikubo, E. Kato, and K. Otsuka, "Sequential production of H2 and CO over supported Ni catalysts," *Fuel,* vol. 83, no. 1, pp. 47-57, 2004.

[7] A. More, C. J. Hansen, and G. Veser, "Production of inherently separated syngas streams via chemical looping methane cracking," *Catalysis Today,* vol. 298, pp. 21-32, 2017.

[8] H. C. Mantripragada and G. Veser, "Intensifying chemical looping dry reforming: Process modeling and systems analysis," *Journal of CO2 Utilization,* vol. 49, 2021.

[9] J. Fang *et al.*, "Efficient hydrogen production system with complementary utilization of methane and full-spectrum solar energy," *Energy Conversion and Management,* vol. 283, May 2023, Art. no. 116951.

[10] W. J. Qu, H. Hong, Q. Li, and Y. M. Xuan, "Co-producing electricity and solar syngas by transmitting photovoltaics and solar thermochemical process," *Applied Energy,* vol. 217, pp. 303-313, May 2018.

[11] J. Fang *et al.*, "Thermodynamic evaluation of a concentrated photochemical-photovoltaic-

thermochemical (CP-PV-T) system in the full-spectrum solar energy utilization," *Applied Energy,* vol. 279, Dec 2020, Art. no. 115778.

[12]   T. X. Liu, Q. B. Liu, J. Lei, J. Sui, and H. G. Jin, "Solar-clean fuel distributed energy system with solar thermochemistry and chemical recuperation," *Applied Energy,* vol. 225, pp. 380-391, Sep 2018.

[13]   W. Han, Q. Chen, R.-m. Lin, and H.-g. Jin, "Assessment of off-design performance of a small-scale combined cooling and power system using an alternative operating strategy for gas turbine," *Applied Energy,* vol. 138, pp. 160-168, 2015.

[14]   T. Xie, K.-D. Xu, Y.-L. He, K. Wang, and B.-L. Yang, "Thermodynamic and kinetic analysis of an integrated solar thermochemical energy storage system for dry-reforming of methane," *Energy,* Article vol. 164, pp. 937-950, Dec 1 2018.